

Investigation of C–H...O=C and N–H...O=C hydrogen-bonding interactions in crystalline thymine by DFT calculations of O-17, N-14 and H-2 NQR parameters

Mahmoud Mirzaei^a, Nasser L. Hadipour^{a,*}, Kamran Ahmadi^b

^a Department of Chemistry, Tarbiat Modares University, P.O. Box 14115-175, Tehran, Iran

^b Materials and Energy Research Center (MERC), P.O. Box 14155-4777, Tehran, Iran

Received 9 August 2006; received in revised form 9 October 2006; accepted 12 October 2006

Available online 25 October 2006

Abstract

A computational study at the level of density functional theory (DFT) was carried out to investigate C–H...O=C and N–H...O=C hydrogen-bonding interactions (HBs) in the real crystalline cluster of thymine by O-17, N-14 and H-2 calculated nuclear quadrupole resonance (NQR) parameters. To perform the calculations, a hydrogen-bonded pentameric cluster of thymine was created using X-ray coordinates where the hydrogen atoms positions are optimized and the electric field gradient (EFG) tensors were calculated for the target molecule. Additional EFG calculations were also performed for crystalline monomer and an optimized isolated gas-phase thymine. The calculated EFG tensors at the level of B3LYP and B3PW91 DFT methods and 6-311++G** and CC-pVTZ basis sets were converted to those experimentally measurable NQR parameters, quadrupole coupling constants and asymmetry parameters. The results reveal that because of strong contribution to N–H...O=C HBs, NQR parameters of O₂, N₁ and N₃ undergo significant changes from monomer to the target molecule in cluster. Furthermore, the NQR parameters of O₂ also undergo some changes because of non-classical C–H...O=C HBs.

© 2006 Elsevier B.V. All rights reserved.

Keywords: DFT; NQR; C–H...O=C; N–H...O=C; Hydrogen bond; Thymine

1. Introduction

Hydrogen-bonding interactions (HBs) play a unique role in chemical and biochemical systems, especially between nucleic acids base pairs [1]. The HBs typically have both covalent, electrostatic and dispersion contributions, therefore, electric field gradient (EFG) tensors are very insightful elements to characterize the properties of various HBs types. Electric quadrupole moment of quadrupolar nuclei, nuclei with nuclear spin angular momentum, I , greater than one-half, interact with the EFG tensors arisen at the sites of quadrupolar nuclei. The energy of this interaction is so-called quadrupole coupling constant, C_Q , which can be measured experimentally by either nuclear quadrupole resonance (NQR) spectroscopy or nuclear magnetic resonance (NMR) spectroscopy [2,3]. Another important parameter is asymmetry parameter, η_Q , which measures EFG tensors deviation

from cylindrical symmetry at the site of quadrupolar nucleus. Both of these experimental parameters, C_Q and η_Q , can be reproduced reliably by high-level quantum chemical calculations.

The contribution of thymine, DNA characteristic nucleobase, to HBs has been studied numerous in the literature [4–12]. Wu and co-workers [13,14] either measured experimentally or calculated computationally ¹⁷O NQR parameters of thymine in solid-phase. However, their considered hydrogen-bonded cluster of thymine in the calculations was not complete. Russo and co-workers [15] also performed computational NQR study on thymine but the presence of HBs was not either considered in their EFG tensors calculations. To the best of our knowledge, to this point, no systematic computational NQR study has been reported for thymine in the literature where this kind of study is essential in the interpretation of experimental measurements.

Present work calculates ¹⁷O, ¹⁴N and ²H EFG tensors in the structure of thymine by density functional theory (DFT). Recent studies reveal that to calculate reliable EFG results, the considered model system in calculations must be as much closer to

* Corresponding author. Tel.: +98 21 88011001x3488; fax: +98 21 88009730.

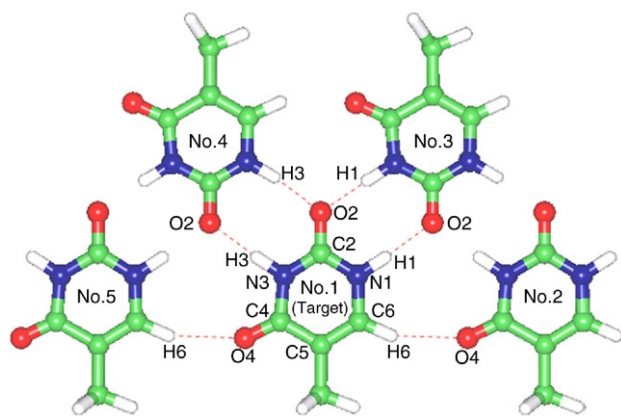
E-mail address: hadipour.n@gmail.com (N.L. Hadipour).

experiment as possible [16–20]. Therefore, the crystalline coordinates of thymine were obtained from X-ray diffraction study [21] and a pentameric cluster was created using these coordinates where hydrogen positions are optimized, see Scheme 1 and Table 1 for details. To determine the influence of HBs on EFG tensors at the sites of various nuclei, the calculated results of monomer and the target molecule in pentameric cluster of thymine were compared. Furthermore, the EFG tensors calculations were also performed for an optimized isolated gas-phase thymine. Tables 2–4 exhibit the converted calculated EFG tensors of ^{17}O , ^{14}N and ^2H nuclei to experimental C_Q and η_Q parameters in three model systems of thymine, optimized isolated gas-phase, crystalline monomer and the target molecule in crystalline pentameric cluster. Table 5 presents ^{17}O , ^{14}N and ^2H EFG tensors orientations in the molecular frame of reference for the target molecule in pentameric cluster of thymine.

2. Computational aspects

All quantum chemical calculations were carried out at the level of density functional theory (DFT) via Gaussian 98 package [22]. The employed DFT methods are B3LYP and B3PW91 [23–25] and the basis sets are 6-311++G** and CC-pVTZ which yield reliable ^{17}O , ^{14}N and ^2H calculated EFG tensors [16,17,26]. Considering the HBs presence in the calculations, pentameric cluster of thymine was created using X-ray coordinates [21], see Scheme 1 and Table 1 for details. Since X-ray diffraction is deficient to locate the accurate hydrogen atoms positions in the crystalline structure, the hydrogen atoms of thymine were optimized at the level of B3LYP/6-311G**. It is noteworthy that the locations of hydrogen atoms were allowed to fully relax whereas those of other atoms were frozen during the optimization. Another optimization at the level of B3LYP/6-311G** was also performed for an isolated gas-phase thymine, see Table 1.

To have a direct relation with the experiment, the calculated EFG tensors eigenvalues in the principal axis system (PAS),



Scheme 1. The pentameric crystalline cluster of thymine. Dash lines show hydrogen-bonding interactions of the target molecule in cluster. The transformed coordinates are: No.1: x ; y ; z , No.2: x ; $y+1$; z , No.3: $-x+1$; $y+1/2$; z , No.4: $-x+1$; $y-1/2$; z , and No.5: x ; $y-1$; z .

Table 1

The structural properties of thymine

Geometrical parameters	Fully optimized isolated gas-phase	Crystalline monomer ^a	Intermolecular HBs ^b	Distances and angles
$r_{\text{N}_1-\text{C}_2}$	1.39 Å	1.31 Å	$r_{\text{N}_1\cdots\text{O}_2}$	2.81 Å
$r_{\text{C}_2-\text{N}_3}$	1.39 Å	1.35 Å	$r_{\text{N}_3\cdots\text{O}_2}$	2.79 Å
$r_{\text{N}_3-\text{C}_4}$	1.41 Å	1.41 Å	$r_{\text{H}_1\cdots\text{O}_2}$	1.80 Å
$r_{\text{C}_4-\text{C}_5}$	1.47 Å	1.48 Å	$r_{\text{H}_3\cdots\text{O}_2}$	1.78 Å
$r_{\text{C}_5-\text{C}_6}$	1.35 Å	1.37 Å	$r_{\text{H}_6\cdots\text{O}_4}$	2.34 Å
$r_{\text{C}_5-\text{O}_2}$	1.21 Å	1.25 Å	$\angle_{\text{N}_1-\text{H}\cdots\text{O}_2}$	173.8°
$r_{\text{C}_4-\text{O}_4}$	1.22 Å	1.19 Å	$\angle_{\text{N}_3-\text{H}\cdots\text{O}_2}$	173.0°
$r_{\text{N}_1-\text{H}_1}$	1.01 Å	1.01 Å	$\angle_{\text{C}_6-\text{H}_6\cdots\text{O}_4}$	156.9°
$r_{\text{N}_3-\text{H}_3}$	1.01 Å	1.01 Å		
$r_{\text{C}_6-\text{H}_6}$	1.08 Å	1.08 Å		
$\angle_{\text{N}_1-\text{C}_2-\text{N}_3}$	112.4°	117.8°		
$\angle_{\text{N}_1-\text{C}_2-\text{O}_2}$	123.2°	121.6°		
$\angle_{\text{O}_2-\text{C}_2-\text{N}_3}$	124.4°	120.5°		
$\angle_{\text{C}_2-\text{N}_3-\text{C}_4}$	128.3°	125.9°		
$\angle_{\text{N}_3-\text{C}_4-\text{C}_5}$	114.5°	114.3°		
$\angle_{\text{N}_3-\text{C}_4-\text{O}_4}$	120.5°	121.2°		
$\angle_{\text{O}_4-\text{C}_4-\text{C}_5}$	125.1°	124.4°		
$\angle_{\text{C}_4-\text{C}_5-\text{C}_6}$	118.2°	118.6°		

^a Crystalline monomer is obtained by X-ray coordinates, however, since the hydrogen positions were not reported by X-ray study, they just hydrogen positions were optimized at the level of B3LYP/6-311G**.

^b See Scheme 1.

$|q_{zz}| > |q_{yy}| > |q_{xx}|$, were converted to quadrupole coupling constant, C_Q , and asymmetry parameter, η_Q , via Eqs. (1)–(2). C_Q means the interaction energy between electric quadrupole moment, eQ , of nucleus and the EFG tensors arisen at the site of quadrupolar nucleus. η_Q measures the EFG tensors deviation from cylindrical symmetry at the site of quadrupolar nucleus. The standard values of quadrupole moment, Q , reported by Pyykkö [27] were used in Eq. (1), $Q(^{17}\text{O})=25.58$ mb, $Q(^{14}\text{N})=20.44$ mb and $Q(^2\text{H})=2.86$ mb. Tables 2, 3, 4 exhibit the converted ^{17}O , ^{14}N and ^2H NQR parameters for a fully optimized isolated gas-phase, crystalline monomer obtained by X-ray coordinates and also optimized hydrogen positions and the target molecule in pentameric crystalline cluster of thymine. ^{17}O , ^{14}N and ^2H EFG tensors orientations in the molecular frame of reference for the target molecule in pentameric cluster of thymine are also presented in Table 5.

$$C_Q = e^2 Q q_{zz} h^{-1} \quad (1)$$

$$\eta_Q = |(q_{xx} - q_{yy}) / q_{zz}| \quad (2)$$

3. Results and discussion

To evaluate ^{17}O , ^{14}N and ^2H EFG tensors, a pentameric crystalline cluster of thymine consisting of the most probable interacting molecules with the target one was created by X-ray coordinates [21] where hydrogen atoms positions are optimized, see Scheme 1 and Table 1 for details. The calculated EFG tensors were converted to those experimentally measurable NQR parameters using Eqs. (1) (2) and the results of an optimized isolated gas-phase, crystalline monomer and the

Table 2
¹⁷O NQR parameters of thymine

Nucleus	Method	Basis Set	C_Q (MHz)			η_Q			Experimental ^a	
			Isolated gas-phase ^b	Monomer ^c	Cluster ^d	Isolated gas-phase ^b	Monomer ^c	Cluster ^d	C_Q (MHz)	η_Q
O ₂	B3LYP	6-311++G**	8.45	8.96	7.50	0.33	0.56	0.99	6.65	1.0
		CC-pVTZ	8.26	8.80	7.17	0.29	0.52	0.99		
	B3PW91	6-311++G**	8.36	8.87	7.45	0.35	0.57	0.96		
		CC-pVTZ	8.18	8.71	7.11	0.30	0.53	0.96		
O ₄	B3LYP	6-311++G**	9.73	9.58	9.41	0.01	0.14	0.08	8.40	0.10
		CC-pVTZ	9.53	9.37	9.13	0.05	0.19	0.11		
	B3PW91	6-311++G**	9.62	9.47	9.30	0.01	0.13	0.06		
		CC-pVTZ	9.42	9.26	9.04	0.03	0.18	0.10		

^a The experimental results are from Ref. [14].

^b A fully optimized isolated gas-phase thymine at the level of B3LYP/6-311G**.

^c Crystalline monomer obtained by X-ray coordinates and also optimized hydrogen positions.

^d The target molecule in cluster.

target molecule in crystalline pentameric cluster of thymine are exhibited in Tables 2, 3, 4. A quick look at the results reveals different HBs effects on the EFG tensors at the sites of various nuclei in crystalline structure of thymine. The following text discusses the calculated results of Tables 1, 2, 3, 4, 5, respectively, where those results of B3LYP/6-311++G** because of the least basis set super position error (BSSE) are referred to [26].

3.1. Comparison of an optimized isolated gas-phase and crystalline monomer thymine

To indicate the influence of HBs on the structural properties, an additional optimization at the level of B3LYP/6-311G** was also performed on an isolated gas-phase thymine, see Table 1. The results reveal that the geometrical parameters of the optimized isolated gas-phase and crystalline thymine are different. Therefore, different ¹⁷O, ¹⁴N and ²H EFG tensors were also calculated for the two structures which reveal the relationship between the NQR parameters and the structural properties which is in agreement with the previous NMR study of Xu and co-workers [28]. Tables 2, 3, 4 exhibit more significant difference of NQR parameters for ¹⁷O nuclei rather than ¹⁴N and ²H nuclei in two model systems of optimized isolated gas-phase and crystalline monomer thymine.

3.2. ¹⁷O electric field gradient tensors

This section will discuss the calculated ¹⁷O EFG tensors, see Table 2. A quick look at the results reveals that ¹⁷O EFG tensors of thymine are influenced by HBs. Thymine has two kinds of oxygen nuclei, O₂: amide type [29] and O₄: urea type [30], where O₄ contributes to two N–H...O=C HBs but O₂ contributes to one C–H...O=C HBs. Because of proper intermolecular O...N distances, $r_{O_4...N3-2}=2.74$ Å and $r_{O_4...N1-3}=2.80$ Å, O₂ of the target molecule contributes to strong N–H...O=C HBs with molecules 3 and 4 in the cluster. Therefore, $C_Q(^{17}O_2)$ reduces 1.46 MHz from monomer to the target molecule in cluster. The significant increment of $\eta_Q(O_2)$ also reveals strong contribution of O₂ to HBs. On the other hand, $C_Q(^{17}O_4)$ undergoes 0.17 MHz reduction from monomer to the target molecule in cluster. Although it is not as significant as that of O₂, but refers to the role of C–H...O=C HBs in the crystalline cluster of thymine.

Previously, Wu and co-workers [14] reported the experimental values of $C_Q(^{17}O)$ for thymine in solid-phase, $C_Q(^{17}O_2)=6.65$ MHz and $C_Q(^{17}O_4)=8.40$ MHz, where the difference between the experimental values of C_Q is up to 2 MHz. Hereby, although the exact values of the calculated C_Q parameters in the cluster, $C_Q(^{17}O_2)=7.50$ and $C_Q(^{17}O_4)=9.41$ MHz, deviate

Table 3
¹⁴N NQR parameters of thymine

Nucleus	Method	Basis set	C_Q (MHz)			η_Q		
			Isolated gas-phase ^a	Monomer ^b	Cluster ^c	Isolated gas-phase ^a	Monomer ^b	Cluster ^c
N ₁	B3LYP	6-311++G**	4.10	3.98	3.08	0.09	0.13	0.53
		CC-pVTZ	3.94	3.81	2.91	0.09	0.14	0.55
	B3PW91	6-311++G**	4.04	3.92	3.06	0.10	0.14	0.53
		CC-pVTZ	3.86	3.74	2.88	0.10	0.16	0.56
N ₃	B3LYP	6-311++G**	3.78	3.70	2.86	0.14	0.05	0.60
		CC-pVTZ	3.61	3.53	2.68	0.13	0.03	0.62
	B3PW91	6-311++G**	3.72	3.64	2.84	0.15	0.06	0.59
		CC-pVTZ	3.54	3.46	2.65	0.14	0.04	0.61

^a A fully optimized isolated gas-phase thymine at the level of B3LYP/6-311G**.

^b Crystalline monomer obtained by X-ray coordinates and also optimized hydrogen positions.

^c The target molecule in cluster.

Table 4
²H NQR parameters of thymine

Nucleus	Method	Basis set	C_Q (kHz)			η_Q		
			Isolated gas-phase ^a	Monomer ^b	Cluster ^c	Isolated gas-phase ^a	Monomer ^b	Cluster ^c
H ₁	B3LYP	6-311++G**	272	270	236	0.18	0.17	0.21
		CC-pVTZ	260	259	223	0.17	0.16	0.20
	B3PW91	6-311++G**	273	271	238	0.18	0.17	0.20
		CC-pVTZ	262	261	225	0.17	0.16	0.19
H ₃	B3LYP	6-311++G**	264	266	229	0.16	0.15	0.20
		CC-pVTZ	253	254	216	0.15	0.14	0.18
	B3PW91	6-311++G**	266	267	231	0.15	0.15	0.19
		CC-pVTZ	255	257	218	0.14	0.14	0.18
H ₆	B3LYP	6-311++G**	211	213	202	0.10	0.10	0.09
		CC-pVTZ	194	196	185	0.09	0.09	0.09
	B3PW91	6-311++G**	212	215	204	0.10	0.09	0.08
		CC-pVTZ	197	199	189	0.09	0.09	0.08

^a A fully optimized isolated gas-phase thymine at the level of B3LYP/6-311G**.

^b Crystalline monomer obtained by X-ray coordinates and also optimized hydrogen positions.

^c The target molecule in cluster.

from the experiments, but the difference between the C_Q of the two oxygen nuclei is in good agreement with the experiment. In the other words, O₂ has the major contribution to the HBs while that of O₄ is minor.

3.3. ¹⁴N electric field gradient tensors

This section focuses on the calculated ¹⁴N EFG tensors, see Table 3. N₁ and N₃ are the two nitrogen atoms of thymine which contribute to N–H...O=C HBs in the crystalline pentameric cluster. N₁ of the target molecule interacts with O₂ of molecule 3, $r_{N_1...O_2-3}=2.81$ Å. Having a proper N...O distance, $C_Q(^{14}N_1)$ reduces 0.9 MHz from monomer to the target molecule in cluster. The other nitrogen of the target molecule, N₃, also interacts with O₂ of molecule 4 with a proper N...O distance, $r_{N_3...O_2-4}=2.79$ Å. Therefore, $C_Q(^{14}N_3)$ reduces 0.84 MHz from monomer to the target molecule in cluster which is also a significant change of ¹⁴N EFG tensors. These significant reductions of $C_Q(^{14}N)$ values and also the significant increments of η_Q values from monomer to the target molecule in cluster reveal the significant contributions of nitrogen nuclei to strong N–H...O=C HBs in the cluster of thymine. Since the chemical environments of these two nitrogen nuclei are different, $C_Q(^{14}N_3)$ shifts to lower-field rather than that of N₁. It is noted that to the best of our knowledge, no experimental ¹⁴N NQR data was available in the literature.

3.4. ²H electric field gradient tensor

Table 4 presents the calculated ²H EFG tensors of thymine. Since the hydrogens of methyl group do not contribute to HBs in the cluster, their neighboring molecules were not considered in the calculations to save time. A quick look at the results reveals the influence of HBs on the EFG tensors at H₁, H₃ and H₆ nuclei in the cluster. H₁ and H₃ are chemically bonded to N₁ and N₃, respectively, and contribute to N–H...O=C HBs whereas H₆ contributes to C–H...O=C HBs in the cluster. As mentioned earlier, O₂ has the major contribution to HBs while

that of O₄ is minor. Similarly, contributing to N–H...O=C HBs with O₂ remarkably influences on the $C_Q(^2H_1)$ and $C_Q(^2H_3)$ in the cluster, $C_Q(^2H_1)$ reduces 34 kHz and $C_Q(^2H_3)$ reduces 23 kHz from monomer to the target molecule in cluster. However, because of poor electron environment of hydrogen nuclei, η_Q increase just up to 0.05 from monomer to the target molecule in cluster. Contributing to C–H...O=C HBs, $C_Q(^2H_3)$ reduces 11 kHz from monomer to the target molecule in cluster where η_Q remains unchanged. The proceeding mentioned trends reveal that H₁ and H₃ have the major role of contribution to HBs in the cluster of thymine whereas that of H₆ is minor. To the best of our knowledge, there is not either any experimental ²H NQR data in the literature.

3.5. EFG tensors orientations in the molecular frame of reference

One of the benefits of high-level quantum chemical calculations is determination of EFG tensors orientations in the molecular frame of reference. Within this study, ¹⁷O, ¹⁴N and ²H EFG tensors orientations in the molecular frame of reference were calculated at the level of B3LYP/6-311++G** for the target molecule in cluster of thymine where α : the orientation of q_{xx} , β : the orientation of q_{yy} and γ : the orientation of q_{zz} , see Table 5. The results reveal that the orientations of O₂ and O₄ do not have

Table 5
 The EFG tensors orientations in the molecular frame of reference^a

Nucleus	α	β	γ
O ₂	100.3°	19.9°	22.6°
O ₄	35.5°	108.3°	60.7°
N ₁	114.4°	155.0°	95.3°
N ₃	90.0°	173.5°	96.5°
H ₁	137.7°	93.3°	132.1°
H ₃	37.5°	93.8°	127.3°
H ₆	63.5°	87.6°	153.3°

^a The values are for the target molecule in cluster at the level of B3LYP/6-311++G**.

any harmony. However, N_1 and N_3 are almost in the same orientation, especially in β and γ . For H_1 , H_3 and H_6 , β s are in the same orientations, but, no harmony could be observed in calculated α s and γ s.

4. Concluding remarks

We calculated ^{17}O , ^{14}N and ^2H EFG tensors in the various structures of thymine, an optimized isolated gas-phase, crystalline monomer, and the target molecule in crystalline pentameric cluster. The calculated results reveal that HBs have different effects on the EFG tensor at ^{17}O , ^{14}N and ^2H nuclei. Contributing to $\text{N}-\text{H}\cdots\text{O}=\text{C}$ HBs, $Q_C(^{17}\text{O}_2)$ shifts to lower-field and also undergoes more significant reduction from monomer to the target molecule in cluster rather than that of O_4 which contributes to $\text{N}-\text{H}\cdots\text{O}=\text{C}$ HBs. However, it is noteworthy that the influence of $\text{N}-\text{H}\cdots\text{O}=\text{C}$ HBs on the EFG tensors at O_4 is not negligible. Both N_1 and N_3 contribute to $\text{N}-\text{H}\cdots\text{O}=\text{C}$ HBs and their NQR parameters undergo significant changes. For hydrogens, H_1 and H_3 have the major contribution to HBs while that of H_6 is minor.

References

- [1] J. Watson, H.C. Crick, Molecular structure of nucleic acids: a structure for deoxyribose nucleic acid, *Nature* 171 (1953) 737–738.
- [2] T.P. Das, E.L. Han, *Nuclear Quadrupole Resonance Spectroscopy*, Academic Press, New York, 1958.
- [3] R.S. Drago, *Physical Methods for Chemists*, 2nd ed. Saunders College Publishing, 1992.
- [4] M. Swart, C.F. Guerra, F.M. Bickelhaupt, Hydrogen bonds of RNA are stronger than those of DNA, but NMR monitors only presence of methyl substituent in uracil/thymine, *J. Am. Chem. Soc.* 126 (2004) 16718–16719.
- [5] P. Jurečka, P. Hobza, True stabilization energies for the optimal planar hydrogen-bonded and stacked structures of guanine-cytosine, adenine-thymine, and their 9- and 1-methyl derivatives: complete basis set calculations at the MP2 and CCSD(T) levels and comparison with experiment, *J. Am. Chem. Soc.* 125 (2003) 15608–15613.
- [6] A. Müller, J.A. Frey, S. Leutwyler, Probing the Watson-Crick, Wobble, and sugar-edge hydrogen bond sites of uracil and thymine, *J. Phys. Chem., A* 109 (2005) 5055–5063.
- [7] A. Müller, S. Leutwyler, Nucleobase pair analogues 2-pyridone-uracil, 2-pyridone-thymine, and 2-pyridone-5-fluorouracil: hydrogen-bond strengths and intermolecular vibrations, *J. Phys. Chem., A* 108 (2004) 6156–6164.
- [8] A. Asensio, N. Kobko, J.J. Dannenberg, Cooperative hydrogen-bonding in adenine-thymine and guanine-cytosine base pairs. Density Functional Theory and Møller-Plesset molecular orbital study, *J. Phys. Chem., A* 107 (2003) 6441–6443.
- [9] M.I. Bugar, D. Dhawan, D. Fiat, ^{17}O and ^{14}N spectroscopy of ^{17}O -labeled nucleic acid bases, *Org. Magn. Reson.* 20 (2005) 184–190.
- [10] M. Hanyu, D. Ninomiya, R. Yanagihara, T. Murashima, T. Miyazawa, T. Yamada, Studies on intramolecular hydrogen bonding between the pyridine nitrogen and the amide hydrogen of the peptide: synthesis and conformational analysis of tripeptides containing novel amino acids with a pyridine ring, *J. Pept. Sci.* 11 (2005) 491–498.
- [11] V.I. Danilov, V.M. Anisimov, N. Kurita, D. Hovorun, MP2 and DFT studies of the DNA rare base pairs: the molecular mechanism of the spontaneous substitution mutations conditioned by tautomerism of bases, *Chem. Phys. Lett.* 412 (2005) 285–293.
- [12] G. Villani, Theoretical investigation of hydrogen transfer mechanism in the adenine-thymine base pair, *Chem. Phys.* 316 (2005) 1–8.
- [13] G. Wu, S. Dong, R. Ida, Solid-state ^{17}O NMR of thymine: a potential new probe to nucleic acid base pairing, *Chem. Commun.* (2001) 891–892.
- [14] G. Wu, S. Dong, R. Ida, N. Reen, A solid-state ^{17}O nuclear magnetic resonance study of nucleic acid bases, *J. Am. Chem. Soc.* 124 (2002) 1768–1777.
- [15] N. Russo, E. Sicilia, M. Toscano, A. Grand, Theoretical prediction of nuclear quadrupole coupling constants of DNA and RNA nucleic acid bases, *J. Mol. Struct.* 563 (2001) 125–134.
- [16] M. Mirzaei, N.L. Hadipour, An investigation of hydrogen-bonding effects on the nitrogen and hydrogen electric field gradient and chemical shielding tensors in the 9-methyladenine real crystalline structure: a density functional theory study, *J. Phys. Chem., A* 110 (2006) 4833–4838.
- [17] R. Ida, M.D. Clerk, G. Wu, Influence of $\text{N}-\text{H}\cdots\text{O}$ and $\text{C}-\text{H}\cdots\text{O}$ hydrogen bonds on the ^{17}O NMR tensors in crystalline uracil: computational study, *J. Phys. Chem., A* 110 (2006) 1065–1071.
- [18] F. Elmi, N.L. Hadipour, A study on the intermolecular hydrogen bonds of α -glycylglycine in its actual crystalline phase using ab initio calculated ^{14}N and ^2H nuclear quadrupole coupling constants, *J. Phys. Chem., A* 109 (2005) 1729–1733.
- [19] S.K. Amini, N.L. Hadipour, F. Elmi, A study of hydrogen bond of imidazole and its 4-nitro derivative by ab initio and DFT calculated NQR parameters, *Chem. Phys. Lett.* 391 (2004) 95–100.
- [20] M. Torrent, D.G. Musaev, K. Morokuma, Calculation of nuclear quadrupole parameters in imidazole derivatives and extrapolation to coenzyme B_{12} . A theoretical study, *J. Phys. Chem., B* 103 (1999) 8618–8627.
- [21] K. Ozeki, N. Sakabe, N. Tanaka, The crystal structure of thymine, *Acta Crystallogr., Sect. B* 25 (1969) 1038–1045.
- [22] M.J. Frisch, G.W. Trucks, H.B. Schlegel, G.E. Scuseria, M.A. Robb, J.R. Cheeseman, V.G. Zakrzewski, J.A. Montgomery Jr., R.E. Stratmann, J.C. Burant, S. Dapprich, J.M. Millam, A.D. Daniels, K.N. Kudin, M.C. Strain, O. Farkas, J. Tomasi, V. Barone, M. Cossi, R. Cammi, B. Mennucci, C. Pomelli, C. Adamo, S. Clifford, J. Ochterski, G.A. Petersson, P.Y. Ayala, Q. Cui, K. Morokuma, D.K. Malick, A.D. Rabuck, K. Raghavachari, J.B. Foresman, J. Cioslowski, J.V. Ortiz, A.G. Baboul, B.B. Stefanov, G. Liu, A. Liashenko, P. Piskorz, I. Komaromi, R. Gomperts, R.L. Martin, D.J. Fox, T. Keith, M.A. Al-Laham, C.Y. Peng, A. Nanayakkara, C. Gonzalez, M. Challacombe, P.M.W. Gill, B. Johnson, W. Chen, M.W. Wong, J.L. Andres, C. Gonzalez, M. Head-Gordon, E.S. Replogle, J.A. Pople, *Gaussian 98*, Gaussian Inc, Pittsburgh, PA, 1998.
- [23] A.D. Becke, Density-functional thermochemistry. III. The role of exact exchange, *J. Chem. Phys.* 98 (1993) 5648–5652.
- [24] C. Lee, W. Yang, R.G. Parr, Development of the Colle-Salvetti correlation-energy formula into a functional of the electron density, *Phys. Rev., B* 37 (1988) 785–789.
- [25] J.P. Perdew, Y. Wang, Accurate and simple analytic representation of the electron-gas correlation energy, *Phys. Rev., B* 45 (1992) 13244–13249.
- [26] M. Mirzaei, F. Elmi, N.L. Hadipour, A systematic investigation of hydrogen-bonding effects on the ^{17}O , ^{14}N , and ^2H nuclear quadrupole resonance parameters of anhydrous and monohydrated cytosine crystalline structures: a density functional theory study, *J. Phys. Chem., B* 110 (2006) 10991–10996.
- [27] P. Pykkö, Spectroscopic nuclear quadrupole moment, *Mol. Phys.* 99 (2001) 1617–1629.
- [28] X.-P. Xu, S.C.F. Au-Yeung, Investigation of chemical shift and structure relationships in nucleic acids using NMR and density functional theory methods, *J. Phys. Chem., B* 104 (2000) 5641–5650.
- [29] K. Yamada, S. Dong, G. Wu, Solid-state ^{17}O NMR investigation of the carbonyl oxygen electric-field-gradient tensor and chemical shielding tensor in amides, *J. Am. Chem. Soc.* 122 (2000) 11602–11609.
- [30] S. Dong, R. Ida, G. Wu, A combined experimental and theoretical ^{17}O NMR study of crystalline urea: an example of large hydrogen-bonding effects, *J. Phys. Chem., A* 104 (2000) 11194–11202.